Author/s:
Rousset, E;Gable, RW;Starikova, A;Boskovic, C

Title:
Tetrahalocatecholate Rare Earth Complexes: Dinuclear Motifs with Intramolecular RE···XC(Ar) Interactions

Date:
2020-05-06

Citation:
Rousset, E., Gable, R. W., Starikova, A. & Boskovic, C. (2020). Tetrahalocatecholate Rare Earth Complexes: Dinuclear Motifs with Intramolecular RE···XC(Ar) Interactions. Crystal Growth and Design, 20 (5), pp.3396-3405. https://doi.org/10.1021/acs.cgd.0c00185.

Persistent Link:
https://hdl.handle.net/11343/333725

Tetrahalocatecholate Rare Earth Complexes: Dinuclear Motifs with Intramolecular RE···XC(Ar) Interactions

Elodie Rousset[†], Robert W. Gable[†], Alyona Starikova[‡], Colette Boskovic[*,†]*

† School of Chemistry, University of Melbourne, Victoria 3010, Australia

‡ Institute of Physical and Organic Chemistry, Southern Federal University, 344090 Rostov-on-Don, Russian Federation

ABSTRACT

The reaction of yttrium or cerium nitrate and tetrachloro- or tetrabromocatecholate (X_4Cat^{2-} with X = Cl or Br) has afforded the compounds: $(Et_3NH)_2[\{Y(Cl_4Cat)(H_2O)_2\}_2(\mu\text{-}Cl_4Cat)_2]\cdot 2MeOH\cdot 2H_2O$ (**1-Cl**), $(Et_3NH)_2[\{Y(Br_4Cat)(H_2O)_2\}_2(\mu\text{-}Br_4Cat)_2]\cdot 1.5MeCN$ (**1-Br**), $(Et_3NH)_4[(Cl_4Cat)(H_2O)_2Y(\mu\text{-}Cl_4Cat)_2Y(Cl_4Cat)_2]\cdot 2.5MeOH\cdot 3.5H_2O$ (**2-Cl**), $(Et_3NH)_4[\{Y(Cl_4Cat)(Cl_4CatH)(H_2O)\}_2(\mu\text{-}Cl_4Cat)_2]\cdot 4H_2O$ (**3-Cl**), $(Et_3NH)_7[\{Ce^{IV}(Cl_4CatH)(NO_3)(\mu_2\text{-}Cl_4Cat)_3\}_2Ce^{III}](NO_3)_2$ (**4-Cl)** and $(Et_3NH)_4[Ce^{IV}(X_4Cat)_4]$ (**5-X** with X = Cl, Br). Small variations of the reaction stoichiometry and crystallization methods allow the isolation of dinuclear yttrium complexes with four, five and six tetrachlorocatecholate ligands in **1-Cl**, **2-Cl** and **3-Cl**, respectively. Single crystal X-ray diffraction studies of these compounds reveal a conserved tetrachlorocatecholate-bridged dinuclear yttrium core in each case, but with different peripheral ligation. A key feature of the core unit is Y···ClC(Ar) intramolecular interactions with a catecholate chloro substituent *ortho* to one of the coordinating oxygen atoms. The tetrabromocatecholate analog **1-Br** has also been obtained. Applying similar methods to redox-active cerium, rather than yttrium, instead affords an unusual mixed-valence trinuclear $\{Ce^{III}Ce^{IV}_2\}$ complex in **4-Cl**, as well as two mononuclear cerium(IV) complexes in **5-Cl** and **5-Br**. Density functional theory calculations confirmed the $[Ce^{IV}(Cl_4Cat)_4]^{4-}$ charge distribution for **5-Cl**.

INTRODUCTION

New complexes of rare earth (RE) metals ions are sought after for a range of applications that make use of the unique electronic properties of their ions.[1,2] One of the most important applications of rare earth compounds is employment of cerium oxide in catalytic converters, which makes use of the Ce^{IV}/Ce^{III} redox couple to oxidize CO and NO_x emissions in the exhaust gases from motor vehicles. Cerium species are also widely used in other types of redox-catalysis,[3] while complexes of other rare earth ions play important roles in catalysing organic transformations.[4–6] High quantum yield efficiency and long-lived emissive excited states confer on some rare earth complexes potential applications in new optical technologies, as well as medical diagnostics.[7,8] Other rare earth complexes exhibit the large magnetic moments and magnetic anisotropy that induce single-molecule magnet (SMM) behavior, with resulting possible applications in high density data storage, quantum computing or molecular spintronics.[9–11]

Typically existing in the trivalent state, rare earth ions are hard Lewis acids that tend to coordinate to hard donor atoms though essentially electrostatic interactions. Their considerable lability can pose synthetic challenges over controlling the reaction products, which is often overcome by using high denticity ligands. Nice examples are the robust and stable gadolinium complexes of octadentate ligands employed commercially as MRI contrast agents.[12,13] In contrast, the use of lower denticity ligands can afford an array of different products, including discrete polynuclear complexes and coordination polymers. This is exemplified by the extensive carboxylate chemistry of rare earths.[14,15]

We have an ongoing interest in the chemistry of *o*-dioxolene ligands, which are, in principle, excellent bidentate ligands for rare earth metals. The coordination chemistry of rare earth metals and dioxolene ligands is relatively unexplored and has mainly made use of 3,5- and 3,6-di-

tert-butyl substituted catecholate and semiquinonate,[16–24] with only a few complexes reported for other dioxolenes.[25–29] Our focus has been the lesser used tetrahalo-substituted dioxolenes, with which we have recently developed new SMMs by combining tetrachloro- and tetrabromocatecholate ligands with 18-crown-6 and suitable rare earth metal ions.[30] An important potential advantage of halo-substituted dioxolene ligands is the removal of C-H vibrations that quench the luminescence of emitting lanthanoid species, as well as the possibility of additional intramolecular rare earth-halogen interactions that can engender particular structural moieties. Such interactions are well known in rare earth complexes with fluoro-substituents,[31–35] but there is only a single report of an analogous interaction with other halogens. Chloro-substituted amino-bis(phenol) complexes of yttrium exhibit distinct intramolecular Y···ClC(Ar) interactions with a chloro group *ortho* to the coordinated phenoxo oxygens.[36] These interactions are better known for metals that are not rare earths, for example silver tetrachloro- and tetrabromocatecholate complexes involve important Ag···XC(Ar) (X = Cl, Br) interactions with the halo-substituent *ortho* to the coordinated phenoxo oxygen.[37]

Herein we report the results of our exploration of the chemistry of tetrachloro- and tetrabromo-catecholate with yttrium(III). Weak intramolecular Y···XC(Ar) interactions are an important structural feature, facilitating the formation dinuclear products. The choice of yttrium for this work is based on its capacity as a less expensive and diamagnetic model for the mid to late lanthanoids due to the similarity in ionic radii. In contrast, cerium differs from the other rare earth metals in the relative availability of the tetravalent oxidation state and resulting accessibility of redox chemistry.[38] The ionic radius of cerium(III) is also around 10 % larger than yttrium and the later lanthanoid(III) ions. We also report how the different properties of cerium versus yttrium

afforded different products when the synthetic methods that generated the dinuclear yttrium complexes were extended to cerium.

EXPERIMENTAL SECTION

Synthesis. Tetrabromocatechol was synthesized as previously reported.[39] All other chemicals were purchased from commercial suppliers and used without further purification. Once formed, the yttrium compounds decompose after a day or two when removed from the mother liquor and exposed to air, undergoing color change and loss of crystallinity. Thus, upon isolation, samples for elemental analysis were immediately sealed in ampoules under nitrogen.

$(Et_3NH)_2[\{Y(Cl_4Cat)(H_2O)_2\}_2(\mu\text{-}Cl_4Cat)_2]\cdot 2MeOH\cdot 2H_2O$ (1-Cl). A stoichiometric amount of tetrachlorocatechol (4 eq., 2.08×10^{-4} mol) was deprotonated with two equivalents of triethylamine (Et_3N) per equivalent of ligand in methanol (3 mL) and added dropwise to a solution of $Y(NO_3)_3\cdot xH_2O$ (2 eq., 1.04×10^{-4} mol) in methanol (2 mL). The resulting solution was left to stand at room temperature in the dark. Any amorphous solid that formed was removed by filtration daily, and after no more precipitate was evident, the resulting solution was left to evaporate. After about two weeks, crystals of **1-Cl** could be selected from a mixture of **2-Cl** and **3-Cl** and amorphous material. Samples for crystallography were maintained in contact with the mother liquor to prevent solvent loss.

$(Et_3NH)_2[\{\{Y(Br_4Cat)(H_2O)_2\}_2(\mu\text{-}Br_4Cat)_2]\cdot 1.5MeCN$ (1-Br). A stoichiometric amount of tetrabromocatechol (4 eq., 2.08×10^{-4} mol) was deprotonated with two equivalents of Et_3N per equivalent of ligand in acetonitrile (3 mL) and added dropwise to a solution of $Y(NO_3)_3\cdot xH_2O$ (2 eq., 1.04×10^{-4} mol) in acetonitrile (2 mL). Any precipitate was removed by filtration and the resulting solution was left to stand at room temperature in the dark. Yellow plate-shaped crystals

form after one or two days. The crystals were collected by filtration, washed with cold acetonitrile and diethyl ether, and air-dried. Yield ~30%. Anal. Calcd for $Y_2C_{39}H_{44.5}Br_{16}N_{3.5}O_{12}$: C, 21.19; H, 2.02; N, 2.22. Found: C, 21.37; H, 1.73; N, 2.37.

$(Et_3NH)_4[(Cl_4Cat)(H_2O)_2Y(\mu\text{-}Cl_4Cat)_2Y(Cl_4Cat)_2]\cdot 2.5MeOH\cdot 3.5H_2O$ (2-Cl). Tetrachlorocatechol (6 eq., 1.57×10^{-4} mol) was deprotonated with two equivalents of Et_3N per equivalent of ligand in methanol (2 mL) and added dropwise to a solution of $Y(NO_3)_3\cdot xH_2O$ (2 eq., 5.22×10^{-5} mol) in methanol (1 mL). The resulting solution was left to stand at room temperature in the dark. A mixture of needle-shaped crystals of **2-Cl** and **3-Cl** were always obtained and it was not possible to synthesize a homogeneous batch of **2-Cl**. Samples for crystallography were maintained in contact with the mother liquor to prevent solvent loss.

$(Et_3NH)_4[\{Y(Cl_4Cat)(Cl_4CatH)(H_2O)\}_2(\mu\text{-}Cl_4Cat)_2]\cdot 4H_2O$ (3-Cl). A small excess of tetrachlorocatechol (8 eq., 4.15×10^{-4} mol) was deprotonated with two equivalents of Et_3N in methanol (3 mL) and added dropwise to a solution of $Y(NO_3)_3\cdot xH_2O$ (2 eq., 1.04×10^{-4} mol) in methanol (2 mL). The resulting solution was left to stand at room temperature in the dark. Needle-shaped crystals form after one week. The crystals were collected by filtration, washed with cold methanol and diethyl ether and air-dried. Samples for crystallography were maintained in contact with the mother liquor to prevent solvent loss. Yield: ~40%. The air-dried bulk sample analyzed as desolvated. Anal. Calcd for $Y_2C_{60}H_{70}Cl_{24}O_{14}N_4$: C, 34.32; H, 3.36; N, 2.67. Found: C, 33.62; H, 3.70; N, 3.03.

$(Et_3NH)_7[\{Ce^{IV}(Cl_4CatH)(NO_3)(\mu_2\text{-}Cl_4Cat)_3\}_2Ce^{III}](NO_3)_2$ (4-Cl). Tetrachlorocatechol (5 eq., 2.61×10^{-4} mol) was deprotonated with two equivalents of Et_3N per equivalent of ligand in methanol (3 mL) and added dropwise to a solution of $Ce(NO_3)_3\cdot 6H_2O$ (2 eq., 1.04×10^{-4} mol) in methanol (3 mL) with a drop of water. The resulting solution slowly turned purple after one minute

of stirring, changing to dark black/purple after about three minutes. It was then left to evaporate in the dark. Dark purple block-shaped crystals of **4-Cl** always formed overnight, cocrystallized with an amorphous powder, and it was not possible to isolate a homogenous bulk sample.

General Synthesis of $(Et_3NH)_4[Ce(X_4Cat)_4]$ (5-X). A solution of the tetrahalocatechol (4 eq., 1.84×10^{-4} mmol) deprotonated by 2 equivalents of Et_3N per ligand in methanol (2 mL) was layered over a solution of $Ce(NO_3)_3\cdot6H_2O$ (1 eq., 0.46×10^{-4} mmol) in methanol (1 mL) and stored in the fridge. Dark coloured plate-shaped crystals appeared overnight. They were collected by filtration, washed with cold methanol and diethyl ether and air-dried.

$(Et_3NH)_4[Ce(Br_4Cat)_4]$(5-Br). Crystals were isolated as dark green blocks. Yield: 80 %. Anal. Calcd for $CeC_{48}H_{64}Br_{16}N_4O_8$: C, 25.70; H, 2.88; N, 2.50. Found: C, 25.53; H, 2.72; N, 2.45

$(Et_3NH)_4[Ce(Cl_4Cat)_4]$ (5-Cl). Crystals were isolated as dark purple blocks. Yield: 84 %. Anal. Calcd for $CeC_{48}H_{64}Cl_{16}N_4O_8$: C, 37.62; H, 4.21; N, 3.66. Found: C, 37.77; H, 4.17; N, 3.52.

Crystallography. Apart from **2-Cl**, which was collected at 160 K, the crystallographic data (Table 1) were collected at 130 K from single crystals mounted on a loop fiber using an Oxford Diffraction SuperNova Dual Wavelength single-crystal X-ray diffractometer with Cu Kα radiation (λ = 1.5418 Å). The data were reduced using CrysAlisPro software,[40] using numerical absorption correction based on Gaussian integration over a multifaceted crystal model. Using Olex2,[41] the structures were solved with the ShelXT[42] structure solution program using intrinsic phasing and refined with the ShelXL[43] refinement package using least squares minimization.

All non-hydrogen atoms were refined with anisotropic displacement parameters while hydrogen atoms (including the one on the phenol O atom in **3-Cl**) were placed at calculated positions and refined using the riding model. For **1-Cl** and **3-Cl**, the triethylammonium cations were highly disordered and attempts to adequately model these were unsuccessful. Accordingly,

the refinement was carried out with the OLEX2 Solvent Mask routine to account for the contribution of the disordered cations to the structure. For **2-Cl,** one water molecule was disordered over two positions, one methanol molecule was disordered over two positions and one of the solvent molecules appeared to be a mixture of water and methanol; for the latter refinement was carried with the occupancies of the two molecules being fixed at 0.5.

Table 1. Crystallographic data for Compounds **1-Cl**, **2-Cl**, **3-Cl**, **4-Cl**, **5-Cl** and **5-Br**

	1-Cl	**2-Cl**	**3-Cl**	**4-Cl**	**5-Cl**	**5-Br**
Empirical formula	$Y_2C_{38}H_{52}Cl_{16}N_2O_{16}$	$Y_2C_{56.5}H_{85}Cl_{20}N_4O_{18}$	$Y_2C_{60}H_{78}Cl_{24}N_4O_{18}$	$Ce_3C_{90}H_{114}Cl_{32}N_{11}O_{28}$	$CeC_{48}H_{64}Cl_{16}N_4O_8$	$CeC_{48}H_{64}Br_{16}N_4O_8$
Formula weight	1537.83	1995.10	2171.88	3352.68	1532.35	2243.71
Temperature/K	130.10(10)	159.31(10)	130.00(10)	130.00(10)	130.01(10)	130.01(10)
Crystal system	*triclinic*	*monoclinic*	*monoclinic*	*orthorhombic*	*monoclinic*	*monoclinic*
Space group	*P*-1	$P2_1/c$	$P2_1$	*Pbca*	*C2/c*	*C2/c*
a/Å	9.4133(5)	26.7260(3)	12.76201(16)	24.0900(3)	20.3453(5)	20.5008(2)
b/Å	11.9073(6)	15.51780(10)	28.0044(4)	17.98638(18)	15.0539(4)	15.31560(10)
c/Å	15.1996(8)	20.6321(3)	12.8287(2)	30.0558(4)	20.2968(7)	20.6991(2)
α/°	85.004(4)	90	90	90	90	90
β/°	87.288(4)	94.5220(10)	104.8176(14)	90	94.513(2)	94.5920(10)
γ/°	88.812(4)	90	90	90	90	90
V/Å^3	1695.07(15)	8530.09(17)	4432.39(11)	13023.0(3)	6197.2(3)	6478.28(10)
Z	1	4	2	4	4	4
ρ_{calc} g/cm^3	1.507	1.554	1.447	1.71	1.642	2.300
μ/mm^{-1}	8.560	8.098	8.84	14.6	12.459	17.411
F(000)	772	4056	1916	6692	3096.0	4248.0
Crystal size/mm^3	0.203×0.104×0.064	0.166×0.153×0.071	0.143×0.107×0.018	0.134×0.129×0.056	0.464×0.067×0.061	0.396×0.169×0.119
Radiation	CuKα (λ = 1.54184)	CuKα (λ = 1.54184)	CuKα (λ = 1.54184)	CuKα (λ = 1.54184)	CuKα (λ = 1.54184)	CuKα (λ = 1.54184)
2Θ range for data collection/°	9.07 to 151.522	6.592 to 151.598	7.128 to 151.302	5.882 to 151.464	7.314 to 154.456	7.214 to 154.254
Index ranges	$-11 \le h \le 11$, $-12 \le k \le 14$, $-12 \le l \le 18$	$-31 \le h \le 33$, $-19 \le k \le 16$, $-18 \le l \le 25$	$-15 \le h \le 15$, $-34 \le k \le 35$, $-16 \le l \le 14$	$-30 \le h \le 30$, $-22 \le k \le 15$, $-37 \le l \le 37$	$-23 \le h \le 25$, $-14 \le k \le 19$, $-25 \le l \le 25$	$-25 \le h \le 25$, $-19 \le k \le 17$, $-26 \le l \le 25$
Reflections collected	11945	63607	32590	95918	31626	48255
Independent reflections	6793 [R_{int} = 0.0467, R_σ = 0.0663]	17487 [R_{int} = 0.0970, R_σ = 0.0739]	15824 [R_{int} = 0.0491, R_σ = 0.0658]	13462 [R_{int} = 0.0626, R_σ = 0.0376]	6514 [R_{int} = 0.0397, R_σ = 0.0293]	6853 [R_{int} = 0.0562, R_σ = 0.0329]
Data/restraints /parameters	6793/10/284	17487/106/1018	15824/18/852	13462/0/785	6514/0/354	6853/0/354
Goodness-of-fit on F^2	1.001	1.022	1.003	1.01	1.059	1.147
Final *R* indexes [$I \ge 2\sigma(I)$]	R_1 = 0.0446, wR_2 = 0.1198	R_1 = 0.0669, wR_2 = 0.1804	R_1 = 0.0423, wR_2 = 0.1042	R_1 = 0.0373, wR_2 = 0.0951	R_1 = 0.0277, wR_2 = 0.0747	R_1 = 0.0335, wR_2 = 0.0872
Final *R* indexes [all data]	R_1 = 0.0522, wR_2 = 0.1257	R_1 = 0.0789, wR_2 = 0.1957	R_1 = 0.0476, wR_2 = 0.1081	R_1 = 0.0473, wR_2 = 0.103	R_1 = 0.0284, wR_2 = 0.0755	R_1 = 0.0336, wR_2 = 0.0873
Largest diff. peak/hole / e Å^{-3}	1.12/-0.96	1.94/-1.65	0.80/-0.93	1.48/-0.84	0.47/-1.15	1.26/-2.03

Powder X-Ray Diffraction. P-XRD data were collected on a Rigaku Oxford Diffraction SuperNova Dual Wavelength single crystal X-ray diffractometer using Cu-Kα radiation at 130 K. Powder samples were prepared by gently grinding a few crystals of the bulk samples and loading the resulting micro-crystalline powder samples in glass capillaries for measurement. Data were collected in the 6 to 60° 2θ range with an exposure time of 60 s per frame.

Elemental analyses were performed at Campbell Microanalytical Laboratory, University of Otago, Dunedin, New Zealand.

Density Functional Theory Calculations. Density functional theory (DFT) calculations were performed using the Gaussian 16[44] program packages with UB3LYP/6-311++G(d,p)/SDD approximation. The extended 6-311++G(d,p) basis set was used for all atoms with the exception of cerium, for which SDD basis set and the effective core potential were employed. The stationary points on the potential energy surfaces were located by full geometry optimization and checked for the stabilities of the DFT wave function. Exchange coupling of unpaired electrons in the paramagnetic centers was estimated using the "broken symmetry" (BS) approach.[45] The exchange coupling constant J (in cm^{-1}; $\hat{H} = -2JS_1 \cdot S_2$) was calculated with the use of Yamaguchi equation.[46]

RESULTS AND DISCUSSION

Synthesis. The reaction of yttrium(III) nitrate with various amounts of tetrahalocatecholate X_4Cat^{2-} ligands, deprotonated with triethylamine, leads to a series of dinuclear compounds (Scheme 1) of general formula $(Et_3NH)_a[Y_2(X_4Cat)_b(X_4CatH)_c(H_2O)_d(\mu_2\text{-}X_4Cat)_2]$ ($\{Y_2(X_4Cat)_{2+b+c}\}$). As reported previously for compounds containing similar ligands, the bromocatecholate analogues are yellow, while the chlorocatecholate complexes are colorless.[30] Varying the equivalents of catechol employed in the synthesis, from four to eight per two

yttrium(III) ions, affords a conserved $\{Y_2(\mu\text{-}X_4Cat)_2\}$ core for all complexes. The two catecholate ligands behave as bis-bidentate ligands, with one catecholate oxygen atom bridging the two metal centers. Key to the robustness of the core is an intramolecular Y···XC(Ar) interaction with the halo-substituent *ortho* to the bridging catecholate oxygen atom. Although the dinuclear species possess the same core structure, they exhibit variability in the completion of the yttrium coordination spheres, depending on the amount of tetrahalocatecholate available in the reaction. We have identified distinct complexes with three different Y:X_4Cat ratios: $\{Y_2(X_4Cat)_4\}$ (**1-X**), $\{Y_2(X_4Cat)_5\}$ (**2-X**) and $\{Y_2(X_4Cat)_6\}$ (**3-X**) where X = Cl or Br in the compounds $(Et_3NH)_2[\{Y(Cl_4Cat)(H_2O)_2\}_2(\mu\text{-}Cl_4Cat)_2]\cdot 2MeOH\cdot 2H_2O$ (**1-Cl**), $(Et_3NH)_2[\{Y(Br_4Cat)(H_2O)_2\}_2(\mu\text{-}Br_4Cat)_2]\cdot 1.5MeCN$ (**1-Br**), $(Et_3NH)_4[(Cl_4Cat)(H_2O)_2Y(\mu\text{-}Cl_4Cat)_2Y(Cl_4Cat)_2]\cdot 2.5MeOH\cdot 3.5H_2O$ (**2-Cl**) and $(Et_3NH)_4[\{Y(Cl_4Cat)(Cl_4CatH)(H_2O)\}_2(\mu\text{-}Cl_4Cat)_2]\cdot 4H_2O$ (**3-Cl**).

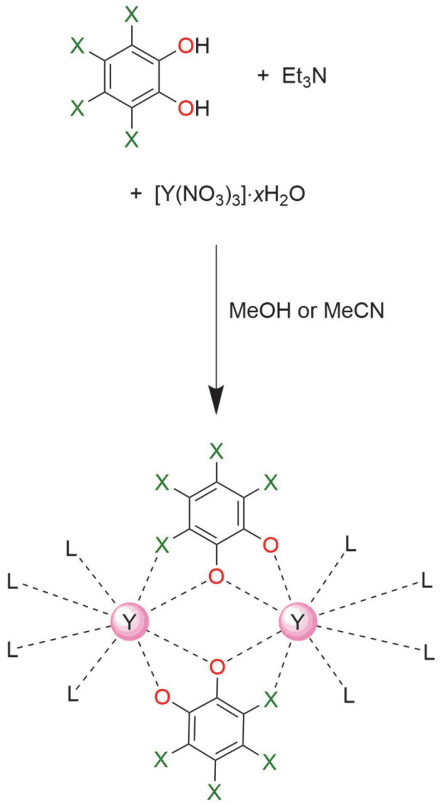

Scheme 1. General synthetic pathway for the formation of the dinuclear species $[Y_2(X_4Cat)_b(X_4CatH)_c(H_2O)_d(\mu\text{-}X_4Cat)_2]^{n-}$ (**1-X**, **2-X** and **3-X**; X = Cl, Br; L = X_4Cat^{2-}, X_4CatH^-, or H_2O).

The reaction conditions for the formation of complexes with different metal to ligand ratios are very similar and mixtures of the different species are often obtained. We focused our attention on the challenge of selectively forming pure samples of the different complexes. This was achieved, in part, by taking advantage of the subtle differences in the solubility of chloro- versus bromocatecholate complexes.[30] The lower solubility of the tetrabromocatecholate compounds allows overnight crystallization of pure $\{Y_2(Br_4Cat)_4\}$ (**1-Br**) family, whereas the greater solubility of the tetrachlorocatecholate compounds affords the formation of pure $\{Y_2(Cl_4Cat)_6\}$ (**3-**

Cl) after one week. The reaction conditions were carefully optimized to try to access homogeneous samples of these compounds in reasonable yield. An analytically pure and homogeneous bulk sample of **1-Br** can be obtained using a stoichiometric amount of tetrabromocatechol and stopping the crystallization after the appearance of the first crystals, although the crystals are too poorly diffracting to afford a good data set. A pure bulk sample of compound **3-Cl** is obtained using an excess of tetrachlorocatechol and removing the first non-crystalline products obtained overnight, then collecting the desired compound after one week. Compounds **1-Br** and **3-Cl** can both be obtained in moderate yield. Efforts to measure powder diffraction patterns of the bulk samples of **1-Br** and **3-Cl** were unsuccessful, as grinding the crystals inevitably generated amorphous materials. However, in each case, unit cell analyses performed on more than ten individual crystals of each batch are consistent with a homogeneous sample and elemental analyses of the dried samples (immediately sealed under nitrogen) indicate purity.

Crystals of the other combinations $\{Y_2(Cl_4Cat)_4\}$ (**1-Cl**) and $\{Y_2(Br_4Cat)_6\}$ (**3-Br**) can also be obtained, but only as mixtures. Although a good quality crystal structure is reported for **1-Cl**, crystals of **3-Br** were poorly diffracting, and the resulting structure was poorly resolved. The intermediate 2:5 ratio $\{Y_2(X_4Cat)_5\}$ complex (**2-X**) was observed co-crystallizing with **3-X** if insufficient tetrahalocatechol was employed in the reaction for **3-X**. Indeed, it proved impossible to obtain a homogenous batch of either **2-Cl** or **2-Br**, although the use of six equivalents of tetrachlorocatechol reliably affords a reasonable amount of **2-Cl** co-crystallized with **3-Cl**.

The choice of reaction solvent also plays an important role in determining the final product. Carrying out the reaction in methanol affords **2-Cl** and **3-Cl**, both of which feature terminal water ligands. In contrast, the use of methanol for **1-Br** instead generates an equivalent complex with terminal methanol ligands, as indicated by preliminary single crystal X-ray diffraction studies.

Instead, generation of **1-Br**, with four terminal water ligands, requires the use of the more poorly coordinating acetonitrile as solvent.

The similarity of their ionic radii often allows yttrium(III) to be a good substitute for the later lanthanoid(III) ions and isostructural complexes are generally obtained. We have begun to extend the syntheses optimized for yttrium to lanthanoid(III) ions and preliminary studies have afforded equivalent dinuclear complexes for selected lanthanoids ranging in size from neodymium(III) to ytterbium(III), which will be reported in due course. However, cerium has proved to be a notable exception. Our initial efforts with cerium (Scheme S1) to obtain analogous dinuclear cerium(III) complexes instead afforded dark-colored solutions indicative of oxidation to cerium(IV). In lieu of dinuclear species, we obtained crystals of a mixed-valence trinuclear complex in the compound $(Et_3NH)_7[\{Ce^{IV}(Cl_4CatH)(NO_3)(\mu_2\text{-}Cl_4Cat)_3\}_2Ce^{III}](NO_3)_2$ (**4-Cl**), which form together with an amorphous dark-colored powder. Slowing down the crystallization process, by layering methanol solutions of the tetrahalocatecholates and cerium(III) nitrate at 4 °C, instead affords pure samples of the mononuclear compounds $(Et_3NH)_4[Ce^{IV}(X_4Cat)_4]$ (**5-X** with X = Cl, Br) in high yields (Scheme S1). The *in situ* generation of cerium(IV) in **4-Cl** and **5-X** by air oxidation is in contrast to our previous report of cerium(III) complexes of tetrahalocatecholate and 18-crown-6 ligands, although in that case, dark coloration of the mother liquor is indicative of partial oxidation during the reaction.[30] Compounds **5-Cl** and **5-Br** are the only chloro-/bromo-analogs in this work to not require substantial difference in the synthesis and crystallization procedures. In addition, compounds **5-Cl** and **5-Br** are the only compounds to maintain their crystallinity upon grinding, as evident from the powder X-ray diffraction patterns of the bulk samples (Figure S1). The experimental diffractograms are in excellent agreement with those

calculated from the single crystal diffraction data, consistent with the purity and stability of these compounds.

Structure Description. Crystallographic details of compounds **1-Cl**, **2-Cl**, **3-Cl**, **4-Cl**, **5-Cl** and **5-Br** are reported in Table 1 and selected interatomic distances and angles are presented in Tables 2, S1 and S2. The common structural feature of the dinuclear complexes in compounds **1-Cl**, **2-Cl** and **3-Cl** is a core comprised of two yttrium centers and two bridging tetrachlorocatecholate ligands (Figures 1 and S2). Each of the catecholate ligands bridges to yttrium centers through a single oxygen atom, with the other oxygen atom completing the yttrium chelation. The position of the ligand allows the chloro-substituent in the *ortho* to the bridging catecholate oxygen atom to participate in an intramolecular Y···ClC(Ar) interaction with the yttrium center with a Y···Cl distance of around 3.0-3.1 Å for all dinuclear complexes.

Table 2. Selected Interatomic Distances (Å) for **1-Cl**, **2-Cl**, **3-Cl** and **4-Cl**.

	1-Cl	**2-Cl**	**3-Cl**	**4-Cl**	
				Ce(III)	**Ce(IV)**
RE-O (μ_2-Cl_4Cat^{2-})[a]	2.310(2), 2.400(2)	2.330(3)-2.395(3)	2.300(4)-2.432(4)	2.398(3)-2.436(3)	2.459(3)-2.495(3)
RE-O (μ_2-Cl_4Cat^{2-})[b]	2.238(3)	2.244(3), 2.236(3)	2.248(5), 2.240(4)	-	2.252(2)-2.328(2)
RE-O (Cl_4Cat^{2-})[c]	2.263(2), 2.344(2)	2.326(3)-2.344(3)	2.296(5)-2.333(5)	-	-
RE-O (Cl_4CatH^-)	-	-	2.246(5), 2.244(5)	-	2.235(2)
RE-O (H_2O or NO_3)	2.339(3), 2.391(2)	2.323(3), 2.417(3)	2.385(5), 2.415(5)	-	2.620(3), 2.637(3)
RE···Cl	3.096(1)	3.029(1), 3.030(1)	3.116(2), 3.156(2)	3.406(1)-3.650(1)	-
RE···RE[d]	3.812(1)	3.891(5)	3.865(1)	3.753(1)	
RE···RE[e]	6.203(1)	11.544(1)	10.169(8)	10.755(1)	

[a] bridging (Figure S3), [b] terminal, [c] chelating ligand, [d] intramolecular, [e] nearest intermolecular

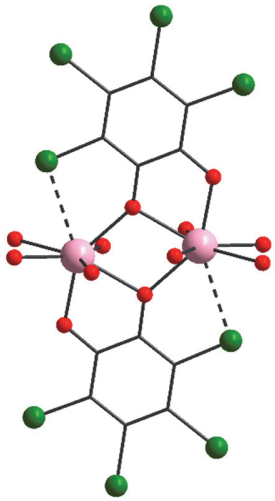

Figure 1. Structural view of the {Y_2(μ-Cl_4Cat)$_2$} core conserved in all dinuclear complexes **1-Cl**, **2-Cl** and **3-Cl**, indicating the important Y···ClC(Ar) interaction. Color code: Y (pink), O (red), C (black), Cl (green); hydrogen atoms omitted for clarity.

Compound **1-Cl** crystallizes as colorless blocks in the triclinic *P*-1 space group. The asymmetric unit contains half a dinuclear species, one disordered Et_3NH^+ countercation, one methanol and one water molecule per yttrium. Crystals were kept in contact with the mother liquor to limit observed very rapid desolvation and loss of quality. The dinuclear yttrium complex features four Cl_4Cat^{2-} and four water ligands (Figure 2). Due to an inversion center, the yttrium centers are crystallographically equivalent. These are 8-coordinate if the Y···ClC(Ar) interaction (Y1···Cl1 = 3.096(1) Å) is included. Continuous shape measures using the program *SHAPE 2.1* (Table S3) for 8-coordinate[47] suggest an intermediate geometry between C_{2v}, a biaugmented trigonal prismatic geometry (BTPR-8, 2.288), and D_{2d}, a square antiprism (SAPR-8, 2.305). The two yttrium centers are separated by 3.812(1) Å. The Y-O distances range from 2.238(3) Å for the terminal oxygen atom of the bridging ligand, to 2.400(2) Å for the bridging oxygen atom. Each of the four Cl_4Cat^{2-} ligands are almost coplanar in two pairs of two and the two planes form an angle of 71.9° (Figure S4). The dinuclear yttrium complexes all pack in the crystal with the same alignment (Figure S5). The nearest intermolecular Y···Y distance is 6.203(1) Å.

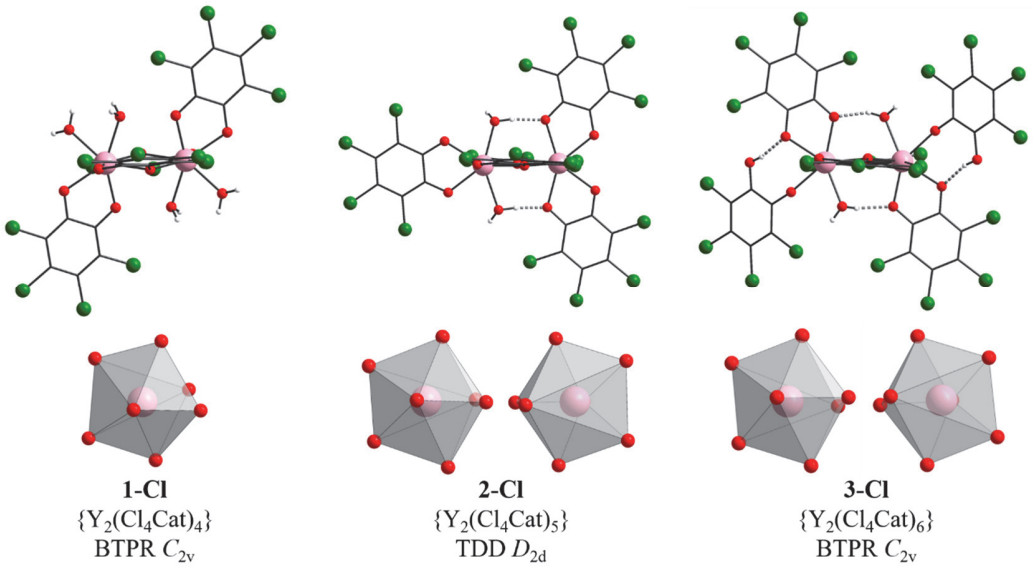

Figure 2. Structural views of the dinuclear complexes in (left to right) **1-Cl**, **2-Cl** and **3-Cl**, the yttrium coordination polyhedra and the associated Shape labels and symmetry point groups.[47]

Compound **3-Cl** crystallizes in the monoclinic $P2_1$ space group with the asymmetric unit comprised of a complete dinuclear species, four Et_3NH^+ countercations and disordered solvent molecules. In this case, the yttrium centers, separated by 3.865(1) Å, are not crystallographically equivalent; however, the geometries around the metallic centers are very similar (Figures 2 and S2). Continuous shape measures (Table S3) reveal C_{2v} symmetries, distorted bioaugmented trigonal prismatic geometries (BTPR-8), with similar indices of 1.896 and 2.526 for Y1 and Y2, respectively, again assuming 8-coordination including the Y···ClC(Ar) interaction (Y···Cl = 3.116(2), 3.156(2) Å). The Y1 center is, however, slightly more distorted than Y2 towards the intermediate geometry between bioaugmented trigonal prismatic and triangular dodecahedron (TDD-8, 2.720). The dinuclear complex in **3-Cl** exhibits an overall $\{Y_2(Cl_4Cat)_6\}$ motif, including the $\{Y_2(\mu\text{-}Cl_4Cat)_2\}$ core evident in **1-Cl**. In addition, each yttrium center is coordinated to a chelating bidentate catecholate and a terminal monoprotonated catecholate. The remaining

coordination site is occupied by a terminal water ligand. The Y-O bond distances are comparable to **1-Cl** and range from 2.240(4) to 2.432(4) Å. An intramolecular hydrogen bond (d(O···O) = 2.668(6) and 2.618(6) Å) is evident between the Cl_4CatH^- phenol group and an oxygen atom from the nearby bidentate Cl_4Cat^{2-} ligand. Each of the four bidentate Cl_4Cat^{2-} ligands are almost coplanar in two pairs of two as per **1-Cl** with the two planes forming an angle of 88.2° (Figure S4). However, the monodentate Cl_4CatH^- ligands deviate from the planes containing the bidentate ligands by around 39° and are almost coplanar with each other. The dinuclear yttrium complexes exhibit two different orientations in the crystal and are arranged in zig-zag chains in the *bc* plane (Figure S6). An extensive hydrogen bonding network is evident involving the Et_3NH^+ countercations and cocrystallized water molecules (Table S2). The nearest intermolecular Y···Y distance is 10.169(8) Å.

Compound **2-Cl** crystallizes in the monoclinic $P2_1/c$ space group with the asymmetric unit comprised of a complete dinuclear species, four Et_3NH^+ countercations and disordered solvent molecules. With a $\{Y_2(Cl_4Cat)_5\}$ ratio intermediate between those of **1-Cl** and **3-Cl**, all the tetrachlorocatecholate ligands are doubly deprotonated and bidentate; the $\{Y_2(\mu\text{-}Cl_4Cat)_2\}$ core evident in **1-Cl** and **3-Cl** is also conserved in **2-Cl**. Unlike the other dinuclear complexes, this one is strictly asymmetric, and the two yttrium centers possess different coordination environments (Figures 2 and S2). For Y1, a chelating bidentate catecholate ligand is aligned with the axis formed by the two yttrium centers and two trans-disposed water ligands complete the coordination sphere. A D_{2d} symmetry is observed, as continuous shape measures (Table S3) indicate a distorted triangular dodecahedral coordination geometry (TDD-8, 1.532). In contrast, Y2 has no water ligands, instead incorporating two bidentate catecholate ligands. Shape measurements (Table S3) again suggest the Y2 coordination geometry (as per Y1 in **3-Cl**) is intermediate between D_{2d} (TDD-

8, 2.164) and C_{2v} symmetry (BTPR-8, 2.315), however, with an opposite trend to **3-Cl**. Similar to **1-Cl**, each bidentate ligand is almost perpendicular to those of the core (83.6 °); however, in the case of **3-Cl**, the two water molecules lie in the plane of the ligand (Figure S4). The Y-O distances are in the range 2.236(3) to 2.395(3) Å and similar to those of **1-Cl** and **3-Cl**. The two Y centers are separated by 3.891(5) Å and the Y···ClC(Ar) distances are 3.030(1) and 3.029(1) Å. Intramolecular hydrogen bonding (d(O···O) = 2.617(5) and 2.579(5) Å) is evident between the water ligands of Y1 and the bidentate catecholate ligands of Y2. Although the crystal packing is similar to **1-Cl**, two different orientations of the dinuclear complex are evident (Figure S7). The nearest intermolecular Y···Y distance is 11.544(1) Å.

The dinuclear complexes in **1-Cl**, **2-Cl** and **3-Cl** each exhibit intramolecular Y···ClC(Ar) interactions involving the chloro substituent *ortho* to the bridging catecholate oxygen atom. The Y···Cl distances of 3.096(1), 3.029(1)/3.030(1), 3.116(2)/3.156(2) Å in **1-Cl**, **2-Cl** and **3-Cl**, respectively, are comparable to literature Y···Cl distances values of 2.97-3.22 Å.[36] Although related {$RE_2(\mu$-diox$)_2$} moieties have been observed previously in a dinuclear rare earth complexes with non-halogenated dioxolene (diox) ligands,[20,22–24,28,29] in the present case the additional Y···ClC(Ar) interaction may confer extra stability on the dinuclear core motif.

Compound **4-Cl** crystallizes in the orthorhombic *Pbca* space group with the asymmetric unit comprised of half of the trinuclear cerium complex, 3.5 Et_3NH^+ countercations and one nitrate counteranion. The cerium complex in **4-Cl** is a linear trinuclear complex with a central cerium atom (Ce2) bridged to each of the other inversion-related cerium atoms (Ce1) via three μ_2-Cl_4Cat^{2-} ligands, giving a Ce1···Ce2 distance of 3.753(1) Å (Figure 3). The coordination sphere of Ce1 is completed by a monodentate Cl_4CatH^- and a chelating nitrate ligand. As per **3-Cl**, an intramolecular hydrogen bond (d(O···O) = 2.72 Å) is evident between the Cl_4CatH^- alcohol group

and a nearby oxygen atom from a μ_2-Cl_4Cat^{2-} ligand. The Ce1 centers are 9-coordinate and continuous shape measures (Table S4) suggest the coordination geometry is best described as C_s muffin geometry (MFF-9, 1.523).[48] The coordination of the central Ce2 atom is best described as 8-coordinate, including six oxygens from bridging catecholate ligands (d(Ce-O) = 2.398(3)-2.436(3) Å). There are also two Ce···ClC(Ar) interactions, which at 3.406(1) A are longer than the Y···ClC(Ar) interactions evident in the dinuclear yttrium complexes. Continuous shape measures (Table S3) suggest that the coordination geometry of Ce2 is best described as a highly distorted O_h cubic geometry (CU-8, 8.110).[47] Charge compensation suggests a $Ce^{III}Ce^{IV}_2$ mixed-valence compound, confirmed by bond valence sum calculations consistent with trivalent Ce2 and tetravalent Ce1 (Table S5). Although a number of extended cerium compounds are known to exhibit mixed-valency, mixed-valence discrete complexes are rare.[49] The oxygen atom-bridged linear trinuclear core of **4-Cl** is reminiscent of two 1,4-bis(3,5-dimethylpyrazol-1-yl)cyclohex-2,5-diene-1,4-diolato-bridged cerium complexes reported previously,[50] although in that case all cerium ions are trivalent.

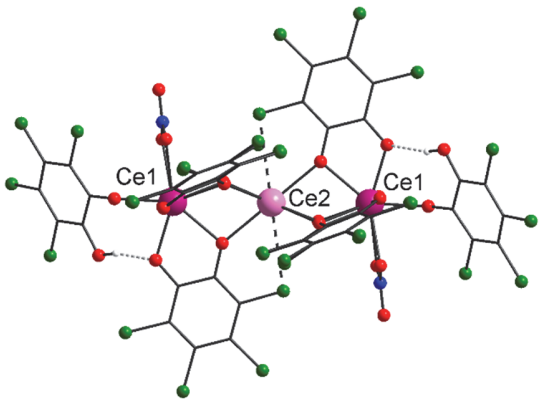

Figure 3. Molecular structure of the trinuclear complex in **4-Cl**; color code as per Figure 2 and Ce^{IV} (dark pink), Ce^{III} (light pink) and nitrogen (blue).

Compound **4-Cl** also exhibits a number of intermolecular N-H···O hydrogen bonds between trethylammonium countercations and the nitrate ligands and non-coordinating anions (Table S2). The complexes stack in a parallel fashion in columns along the *a*-axis, with neighboring columns exhibiting opposing orientations, which is the origin of the zig-zag chain arrangement along the *b*-axis. (Figure S8).

Compounds **5-Cl** and **5-Br** are isomorphous and crystallize in the monoclinic *C*2/*c* space group with half the mononuclear cerium complex and 2 Et_3NH^+ cations in the asymmetric unit. The cerium complex contains four chelating tetrahalocatecholate ligands (Figures 4 and S9). The tetravalent oxidation states of the cerium centers were confirmed again by BVS analysis (Table S5). Continuous shape measures of the complexes in **5-Cl** and **5-Br** indicate D_{2d} symmetry triangular dodecahedral geometries with TDD-8 indices of 1.413 and 1.590 for **5-Cl** and **5-Br**, respectively (Table S3).[47] Similar dodecahedral coordination geometries were also previously reported for two essentially isostructural cerium(IV) complexes with other catecholate ligands.[25,26] The Ce-O distances are in the range 2.353(2)-2.391(2) Å. The dioxolene C-O distances range from are 1.311(4) to 1.334(4) Å and the C-C distances range from 1.381(5) to 1.436(5) Å. These values are consistent with the catecholate oxidation state and, in particular, alternating short and long C-C bonds are not evident around the ring, which would indicate the semiquinonate state.

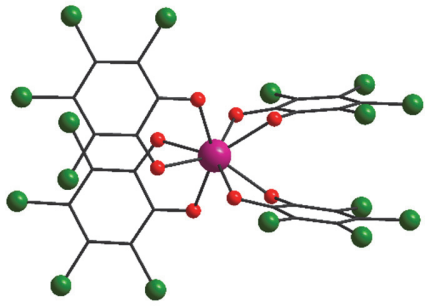

Figure 4. Molecular structure of the complex in **5-Cl**; color code as per Figure 2, Ce^{IV} (dark pink).

Four intermolecular N-H···O hydrogen bonds (Table S2) between the triethylammonium cations and the catecholate oxygen atoms are evident for each cerium complex, with *d*(N···O) = 1.849/1.912 Å and 1.820/1.858 Å for O2/O3 in **5-Cl** and **5-Br**, respectively. The complexes are organized in columns along the *a*- and *c*-axes, separated by a void containing the counterions. Two successive columns are offset, leading to the appearance of dimerization along the *c*-axis. (Figures S10 and S11).

Density Functional Theory Calculations. Although there has been controversy about the cerium oxidation state in organocerium complexes,[51] cerium(IV) complexes with O and N-donor ligands are well-established.[25,26,52–56] The electronic structure is not necessarily straightforward though, particularly in the case of redox-active ligands. Several cerium(IV) complexes exhibit measurable temperature independent paramagnetism due to a multiconfigurational ground state.[56,57] Efforts to measure the magnetic susceptibility of **5-Cl** on a SQUID magnetometer indicated that the sample is diamagnetic at both 2 and 300 K, consistent with a cerium(IV)-catecholate charge distribution. Density functional theory (DFT) calculations of cerium(IV) complexes have become accessible in recent times and have proven useful in understanding the properties of these complexes,[53,55,58,59] so we undertook DFT calculations on **5-Cl** for further clarification of the charge distribution.

An initial geometry optimization using the crystallographic coordinates was performed on the complex in **5-Cl** without countercations on the singlet potential energy surface (PES). It afforded the complex $[Ce^{IV}(Cl_4Cat)_4]^{4-}$ (Table S6) with bond lengths in good agreement with the X-ray data (Figure S12). Geometry optimization of the hypothetical neutral complex $[Ce^{IV}(Cl_4SQ)_4]$ on the quintet PES afforded bond lengths for an analog with

tetrachlorosemiquinonate ligands (Figure S12). Mathematical averaging of the two structures allowed determination of bond lengths for the hypothetical complex $[Ce^{III}(Cl_4SQ)(Cl_4Cat)_3]^{4-}$, which are not in good agreement with the experimental values determined for **5-Cl**. Geometry optimization of this hypothetical molecule on the triplet PES results in a complex (Table S6), in which one unpaired electron is localized on a Ce^{III} ion, while another is delocalized over two tetrachlorodioxolene ligands (Figure 3). As a result, the bond lengths of the four ligands are not equivalent, however still the values are in poorer agreement with the measured X-ray data than those found for the $[Ce^{IV}(Cl_4Cat)_4]^{4-}$ structure. Moreover the calculated $[Ce^{III}(Cl_4SQ)(Cl_4Cat)_3]^{4-}$ is destabilized with respect to the $[Ce^{IV}(Cl_4Cat)_4]^{4-}$ by 6.6 kcal mol^{-1} (Table S6). The search for the broken symmetry state of $[Ce^{III}(Cl_4SQ)(Cl_4Cat)_3]^{4-}$ and the subsequent estimation of exchange coupling constant indicated moderate ferromagnetic exchange interactions ($J = 46$ cm^{-1}) between the cerium(III) ion and another electron delocalized over two dioxolene ligands (Table S6, Figure S12). The calculated triplet state for this complex is inconsistent with the observed diamagnetism of **5-Cl**. Thus, the computational results support the $[Ce^{IV}(Cl_4Cat)_4]^{4-}$ charge distribution for **5-Cl**.

CONCLUDING REMARKS

The controlled synthesis of rare earth complexes with low denticity ligands is challenging because of the lability and coordinative flexibility of rare earth ions. In this work we have employed relatively under-utilized catecholate ligands with halo-substituents and have thereby been able to exploit weak Y···XC(Ar) intramolecular interactions to generate a robust dinuclear yttrium core. We have crystallographically characterized three dinuclear complexes with the same core structure, but different peripheral ligation. Although the initial reaction exploration invariably

generated mixtures of different complexes, through careful control of reaction stoichiometry and crystallization methods we have, in at least some cases, been able to access homogenous and analytically pure bulk samples of a single compound. We thus suggest that the deliberate incorporation into ligands of moieties that can engender secondary interactions may be a useful approach for achieving better control of the synthesis of rare earth complexes with low denticity ligands.

Applying the synthetic methods developed for yttrium to redox-active cerium has instead afforded completely different species: an unusual mixed-valence trinuclear $\{Ce^{III}Ce^{IV}_2\}$ complex and two mononuclear cerium complexes. Density functional theory calculations are consistent with the assignment of the cerium ion as tetravalent in the mononuclear complex, with the four dioxolene ligands in the catecholate state. We have a longstanding interest in magnetic properties and, in ongoing work, we are now applying the synthetic methods we report herein for yttrium and cerium to more magnetically interesting lanthanoid metals. Preliminary observations suggest dinuclear complexes analogous to the present yttrium species are obtained and we will report the results of detailed studies of the magnetic properties of these complexes in due course. We anticipate that the structural fine-tuning enabled by the RE···XC(Ar) intramolecular interactions may facilitate tuning of the magnetic properties.

ASSOCIATED CONTENT

Supporting Information.

The Supporting Information is available free of charge at https://pubs.acs.org/doi/.

Additional synthetic and structural details, powder X-ray diffractograms, structure figures, packing diagrams, results of continuous shape measures and bond valence sum calculations, DFT input and output Cartesian coordinates.

Accession Codes

CCDC 1982497-1982502 contain the supplementary crystallographic data for this paper. These data can be obtained free of charge via www.ccdc.cam.ac.uk/data_request/cif, or by emailing data_request@ccdc.cam.ac.uk, or by contacting The Cambridge Crystallographic Data Centre, 12 Union Road, Cambridge CB2 1EZ, UK; fax: +44 1223 336033.

AUTHOR INFORMATION

Corresponding Author

E-mail: c.boskovic@unimelb.edu.au

ORCID

Elodie Rousset: 0000-0003-3164-6122

Robert W. Gable: 0000-0002-4626-0217

Alyona Starikova: 0000-0001-5842-0559

Colette Boskovic: 0000-0002-1882-2139

Author Contributions

The manuscript was written through contributions of all authors. All authors have given approval to the final version of the manuscript.

Funding Sources

We acknowledge funding from the Australian Research Council, Discovery Project Grant ID: DP150100353.

Notes

The authors declare no competing financial interests.

REFERENCES

(1) Bünzli, J.-C. G. Benefiting from the Unique Properties of Lanthanide Ions. *Acc. Chem. Res.* **2006**, *39*, 53.

(2) Cheisson, T.; Schelter, E. J. Rare Earth Elements: Mendeleev's Bane, Modern Marvels. *Science* **2019**, *363*, 489.

(3) Sridharan, V.; Menéndez, J. C. Cerium(IV) Ammonium Nitrate as a Catalyst in Organic Synthesis. *Chem. Rev.* **2010**, *110*, 3805.

(4) Forsberg, J. H.; Spaziano, V. T.; Balasubramanian, T. M.; Liu, G. K.; Kinsley, S. A.; Duckworth, C. A.; Poteruca, J. J.; Brown, P. S.; Miller, J. L. Use of Lanthanide(III) Ions as Catalysts for the Reactions of Amines with Nitriles. *J. Org. Chem.* **1987**, *52*, 1017.

(5) Edelmann, F. T. Lanthanide Amidinates and Guanidinates in Catalysis and Materials Science: A Continuing Success Story. *Chem. Soc. Rev.* **2012**, *41*, 7657.

(6) Roesky, P. W.; Canseco-Melchor, G.; Zulys, A. A Pentanuclear Yttrium Hydroxo Cluster as an Oxidation Catalyst. Catalytic Oxidation of Aldehydes in the Presence of Air. *Chem. Commun.* **2004**, *4*, 738.

(7) Moore, E. G.; Samuel, A. P. S.; Raymond, K. N. From Antenna to Assay: Lessons Learned in Lanthanide Luminescence. *Acc. Chem. Res.* **2009**, *42*, 542.

(8) Armelao, L.; Quici, S.; Barigelletti, F.; Accorsi, G.; Bottaro, G.; Cavazzini, M.; Tondello, E. Design of Luminescent Lanthanide Complexes: From Molecules to Highly Efficient Photo-Emitting Materials. *Coord. Chem. Rev.* **2010**, *254*, 487.

(9) Escalera-Moreno, L.; Baldovi, J. J.; Gaita-Arino, A.; Coronado, E. Exploring the High-Temperature Frontier in Molecular Nanomagnets: From Lanthanides to Actinides. *Inorg. Chem.* **2019**, *58*, 11883.

(10) Harriman, K. L. M.; Errulat, D.; Murugesu, M. Magnetic Axiality: Design Principles from Molecules to Materials. *Trends Chem.* **2019**, *1*, 425.

(11) Pointillart, F.; Cador, O.; Le Guennic, B.; Ouahab, L. Uncommon Lanthanide Ions in Purely 4f Single Molecule Magnets. *Coord. Chem. Rev.* **2017**, *346*, 150.

(12) Chan, K. W. Y.; Wong, W. T. Small Molecular Gadolinium(III) Complexes as MRI Contrast Agents for Diagnostic Imaging. *Coord. Chem. Rev.* **2007**, *251*, 2428.

(13) Hermann, P.; Kotek, J.; Kubíček, V.; Lukeš, I. Gadolinium(III) Complexes as MRI Contrast Agents: Ligand Design and Properties of the Complexes. *Dalton Trans.* **2008**, *9226*, 3027.

(14) Ouchi, A.; Suzuki, Y.Ohki, Y.; Koizumi, Y. Structure of Rare Earth Carboxylates in Dimeric and Polymeric Forms. *Coord. Chem. Rev.* **1988**, *92*, 29.

(15) Janicki, R.; Mondry, A.; Starynowicz, P. Carboxylates of Rare Earth Elements. *Coord. Chem. Rev.* **2017**, *340*, 98.

(16) Dei, A.; Gatteschi, D.; Pécaut, J.; Poussereau, S.; Sorace, L.; Vostrikova, K. Crystal Field and Exchange Effects in Rare Earth Semiquinone Complexes. *C. R. Acad. Sci. - Ser. IIC Chem.* **2001**, *4*, 135.

(17) Caneschi, A.; Dei, A.; Gatteschi, D.; Massa, C. A.; Pardi, L. A.; Poussereau, S.; Sorace, L. Evaluating the Magnetic Anisotropy in Molecular Rare Earth Compounds . Gadolinium Derivatives with Semiquinone Radical and Diamagnetic Analogues. *Chem. Phys. Lett.* **2003**, *371*, 694.

(18) Caneschi, A.; Dei, A.; Gatteschi, D.; Poussereau, S.; Sorace, L. Antiferromagnetic Coupling between Rare Earth Ions and Semiquinones in a Series of 1:1 Complexes. *Dalton Trans.* **2004**, *24*, 1048.

(19) Claiser, N.; Souhassou, M.; Lecomte, C.; Gillon, B.; Carbonera, C.; Caneschi, A.; Dei, A.; Gatteschi, D.; Bencini, A.; Pontillon, Y.; Lelièvre-Berna, E.. Combined Charge and Spin Density Experimental Study of the Yttrium(III) Semiquinonato Complex $Y(HBPz_3)_2(DTBSQ)$ and DFT Calculations. *J. Phys. Chem. B* **2005**, *109*, 2723.

(20) Kuzyaev, D. M.; Vorozhtsov, D. L.; Druzhkov, N. O.; Lopatin, M. A.; Baranov, E. V.; Cherkasov, A. V.; Fukin, G. K.; Abakumov, G. A.; Bochkarev, M. N. 3,5-Di-*Tert*-Butyl-*o*-Benzoquinone Complexes of Lanthanides. *J. Organomet. Chem.* **2012**, *698*, 35.

(21) Pushkarevsky, N.; Ogienko, M. A.; Smolentsev, A. I.; Novozhilov, I. N.; Witt, A.; Khusniyarov, M. M.; Cherkasov, V. K.; Konchenko, S. N. Cooperative Reduction by Ln^{2+} and Cp*– Ions: Synthesis, Structure, and Magnetic Properties of Sm, Eu, and Yb Complexes with 3,6-Di-*Tert*-Butyl-*o*-Benzoquinone. *Dalton Trans.* **2015**, *45*, 1269.

(22) Klementyeva, S. V.; Smolentsev, A. I.; Abramov, P. A.; Konchenko, S. N. Yttrium 3,5-Di-*Tert*-Butyl-Catecholates Supported by 2,6-Diisopropylphenyl Substituted β-Diketiminate. *Inorg. Chem. Commun.* **2017**, *86*, 154.

(23) Dei, A.; Gatteschi, D.; Massa, C. A.; Pardi, L. A.; Poussereau, S.; Sorace, L. Spontaneous Symmetry Breaking in the Formation of a Dinuclear Gadolinium Semiquinonato Complex: Synthesis, High-Field EPR Studies, and Magnetic Properties. *Chem. Eur. J.* **2000**, *6*, 4580.

(24) Petrov, P. A.; Samsonenko, D. G. Yttrium Complexes with 3,6-Bis(*Tert*-Butylcatecholate). *Russ. J. Coord. Chem.* **2017**, *43*, 500.

(25) Sofen, S. R.; Cooper, S. R.; Raymond, K. N. Crystal and Molecular Structures of Tetrakis(Catecholato)Hafnate(IV) and -Cerate(IV). Further Evidence for a Ligand Field Effect in the Structure of Tetrakis(Catecholato)Uranate(IV). *Inorg. Chem.* **1979**, *18*, 1611.

(26) Haddad, S. F.; Raymond, K. N. The Structure and Properties of Tetrakis(Tironato)Cerate(IV), $Na_{12}[Ce(C_6H_2O_2(SO_3)_2)_4]\cdot 9H_2O\cdot 6C_3H_7NO$. *Inorg. Chim. Acta* **1986**, *122*, 111.

(27) Hickson, J. R.; Horsewill, S. J.; McGuire, J.; Wilson, C.; Sproules, S.; Farnaby, J. H. The Semiquinone Radical Anion of 1,10-Phenanthroline-5,6-Dione: Synthesis and Rare Earth Coordination Chemistry. *Chem. Commun.* **2018**, *54*, 11284.

(28) Raymond, K. N.; Freeman, G. E.; Kappel, M. J. Actinide-Specific Complexing Agents: Their Structural and Solution Chemistry. *Inorg. Chim. Acta* **1984**, *94*, 193.

(29) Freeman, G. E.; Raymond, K. N. Synthetic and Structural Chemistry of Gadolinium and Holmium Catecholates. *Inorg. Chem.* **1985**, *24*, 1410.

(30) Rousset, E.; Piccardo, M.; Boulon, M.-E.; Gable, R.; Soncini, A.; Sorace, L.; Boskovic, C. Slow Magnetic Relaxation in Lanthanoid Crown Ether Complexes: Interplay of Raman and Anomalous Phonon Bottleneck Processes. *Chem. Eur. J.* **2018**, *24*, 14768.

(31) Banerjee, S.; Emge, T. J.; Brennan, J. G. Heterometallic Ln/Hg Compounds with Fluorinated Thiolate Ligands. *Inorg. Chem.* **2004**, *43*, 6307.

(32) Norton, K.; Emge, T. J.; Brennan, J. G. Lanthanide Compounds with Fluorinated OC_6F_5 Ligands: Homo- and Heterovalent Complexes of Eu(II) and Eu(III). *Inorg. Chem.* **2007**, *46*, 4060.

(33) Deacon, G. B.; Forsyth, C. M.; Junk, P. C.; Wang, J. Intramolecular Metal-Fluorocarbon Coordination, C-F Bond Activation and Lanthanoid-Fluoride Clusters with Tethered Polyfluorophenylamide Ligands. *Chem. Eur. J.* **2009**, *15*, 3082.

(34) Deacon, G. B.; Forsyth, C. M.; Junk, P. C.; Kelly, R. P.; Urbatsch, A.; Wang, J. The Effects of Light Lanthanoid Elements (La, Ce, Nd) on (Ar)CF-Ln Coordination and C-F Activation in N,N-Dialkyl-N′-2,3,5,6- Tetrafluorophenylethane-1,2-Diaminate Complexes. *Dalton Trans.* **2012**, *41*, 8624.

(35) Yin, H.; Lewis, A. J.; Carroll, P.; Schelter, E. J. Electrophilic Ln(III) Cations Protected by C-F → Ln Interactions and Their Coordination Chemistry with Weak σ- And π-Donors. *Inorg. Chem.* **2013**, *52*, 8234.

(36) Bouyahyi, M.; Ajellal, N.; Kirillov, E.; Thomas, C. M.; Carpentier, J. F. Exploring Electronic versus Steric Effects in Stereoselective Ring-Opening Polymerization of Lactide and β-Butyrolactone with Amino-Alkoxy- Bis(Phenolate)-Yttrium Complexes. *Chem. Eur.*

J. **2011**, *17*, 1872.

(37) Whitcomb, D. R.; Rajeswaran, M. The First Silver Catechol Complexes: Crystal Structures of Triphenylphosphine Stabilized Silver Tetra-Bromo and Tetra-Chloro-Catechols. *Polyhedron* **2006**, *25*, 2033.

(38) Piro, N. A.; Robinson, J. R.; Walsh, P. J.; Schelter, E. J. The Electrochemical Behavior of Cerium(III/IV) Complexes: Thermodynamics, Kinetics and Applications in Synthesis. *Coord. Chem. Rev.* **2014**, *260*, 21.

(39) Balaydin, H. T.; Akbaba, Y.; Menzek, A.; Şahin, E.; Göksu, S. First and Short Syntheses of Biologically Active, Naturally Occurring Brominated Mono- and Dibenzyl Phenols. *Arkivoc* **2009**, *2009*, 75.

(40) Crysalis Pro, Rigaku Oxford Diffraction. Rigaku Oxford Diffraction: Yarnton 2015.

(41) Dolomanov, O. V.; Bourhis, L. J.; Gildea, R. J.; Howard, J. A. K.; Puschmann, H. OLEX2: A Complete Structure Solution, Refinement and Analysis Program. *J. Appl. Crystallogr.* **2009**, *42*, 339.

(42) Sheldrick, G. M. SHELXT - Integrated Space-Group and Crystal-Structure Determination. *Acta Cryst. A* **2015**, *71*, 3.

(43) Sheldrick, G. M. Crystal Structure Refinement with SHELXL. *Acta Cryst. C* **2015**, *71*, 3.

(44) M. J. Frisch, G. W. Trucks, H. B. Schlegel, G. E. Scuseria, M. A. Robb, J. R. Cheeseman, G. Scalmani, V. Barone, G. A. Petersson, H. Nakatsuji, X. Li, M. Caricato, A. V. Marenich, J. Bloino, B. G. Janesko, R. Gomperts, B. Mennucci, H. P. Hratchian, J. V. Ortiz, A. F. Izmaylov, J. L. Sonnenberg, Williams, F. Ding, F. Lipparini, F. Egidi, J. Goings, B. Peng,

A. Petrone, T. Henderson, D. Ranasinghe, V. G. Zakrzewski, J. Gao, N. Rega, G. Zheng, W. Liang, M. Hada, M. Ehara, K. Toyota, R. Fukuda, J. Hasegawa, M. Ishida, T. Nakajima, Y. Honda, O. Kitao, H. Nakai, T. Vreven, K. Throssell, J. A. Montgomery Jr., J. E. Peralta, F. Ogliaro, M. J. Bearpark, J. J. Heyd, E. N. Brothers, K. N. Kudin, V. N. Staroverov, T. A. Keith, R. Kobayashi, J. Normand, K. Raghavachari, A. P. Rendell, J. C. Burant, S. S. Iyengar, J. Tomasi, M. Cossi, J. M. Millam, M. Klene, C. Adamo, R. Cammi, J. W. Ochterski, R. L. Martin, K. Morokuma, O. Farkas, J. B. Foresman, D. J. Fox. Gaussian 16 (Revision A.03). Gaussian Inc.: Wallingford, CT 2016.

(45) Noodleman, L. Valence Bond Description of Antiferromagnetic Coupling in Transition Metal Dimers. *J. Chem. Phys.* **1981**, *74*, 5737.

(46) Kitagawa, Y.; Saito, T.; Nakanishi, Y.; Kataoka, Y.; Matsui, T.; Kawakami, T.; Okumura, M.; Yamaguchi, K. Spin Contamination Error in Optimized Geometry of Singlet Carbene ($^1A_1$) by Broken-Symmetry Method. *J. Phys. Chem. A* **2009**, *113*, 15041.

(47) Casanova, D.; Llunell, M.; Alemany, P.; Alvarez, S.; D. Casanova, M Llunell, P.; Alemany, S. A. The Rich Stereochemistry of Eight-Vertex Polyhedra: A Continuous Shape Measures Study. *Chem. Eur. J.* **2005**, *11*, 1479.

(48) Ruiz-Martínez, A.; Casanova, D.; Alvarez, S. Polyhedral Structures with an Odd Number of Vertices: Nine-Coordinate Metal Compounds. *Chem. Eur. J.* **2008**, *14*, 1291.

(49) Canaj, A. B.; Siczek, M.; Lis, T.; Murrie, M.; Brechin, E. K.; Milios, C. J. A [Ce_{21}] Keplerate. *Dalton Trans.* **2017**, *46*, 7677.

(50) Werner, D.; Deacon, G. B.; Junk, P. C.; Anwander, R. Pyrazolates Advance Cerium

Chemistry: A Ce ^{III} /Ce ^{IV} Redox Equilibrium with Benzoquinone. *Dalton Trans.* **2017**, *46*, 6265.

(51) Anwander, R.; Dolg, M.; Edelmann, F. T. The Difficult Search for Organocerium(IV) Compounds. *Chem. Soc. Rev.* **2017**, *46*, 6697.

(52) So, Y. M.; Leung, W. H. Recent Advances in the Coordination Chemistry of Cerium(IV) Complexes. *Coord. Chem. Rev.* **2017**, *340*, 172.

(53) Solola, L. A.; Zabula, A. V.; Dorfner, W. L.; Manor, B. C.; Carroll, P. J.; Schelter, E. J. Cerium(IV) Imido Complexes: Structural, Computational, and Reactivity Studies. *J. Am. Chem. Soc.* **2017**, *139*, 2435.

(54) Solola, L. A.; Cheisson, T.; Yang, Q.; Carroll, P. J.; Schelter, E. J. Exploration of the Solid- and Solution-State Structures and Electrochemical Properties of Ce^{IV}(Atrane) Complexes. *Inorg. Chem.* **2018**, *57*, 10543.

(55) Assefa, M. K.; Sergentu, D.; Seaman, L. A.; Wu, G.; Autschbach, J.; Hayton, T. W. Synthesis, Characterization, and Electrochemistry of the Homoleptic f Element Ketimide Complexes $[Li]_2[M(N{=}CtBuPh)_6]$ (M = Ce, Th). *Inorg. Chem.* **2019**, *58*, 12654.

(56) Castro, L.; So, Y.; Cho, C.; Lortz, R.; Wong, K.; Wang, K.; Arnold, P. L.; Au-Yeung, K.; Sung, H. H. -Y.; Williams, I. D.; Leung, W.-H,; Maron, L. A Combined Experimental and Theoretical Study of the Versatile Reactivity of an Oxocerium(IV) Complex: Concerted Versus Reductive Addition. *Chem. Eur. J.* **2019**, *25*, 10834.

(57) Halbach, R. L.; Nocton, G.; Booth, C. H.; Maron, L.; Andersen, R. A. Cerium Tetrakis(Tropolonate) and Cerium Tetrakis(Acetylacetonate) Are Not Diamagnetic but

Temperature-Independent Paramagnets. *Inorg. Chem.* **2018**, *57*, 7290.

(58) Qiao, Y.; Sergentu, D. C.; Yin, H.; Zabula, A. V.; Cheisson, T.; McSkimming, A.; Manor, B. C.; Carroll, P. J.; Anna, J. M.; Autschbach, J.; Shelter, E. J. Understanding and Controlling the Emission Brightness and Color of Molecular Cerium Luminophores. *J. Am. Chem. Soc.* **2018**, *140*, 4588.

(59) Berryman, V. E. J.; Whalley, Z. J.; Shephard, J. J.; Ochiai, T.; Price, A. N.; Arnold, P. L.; Parsons, S.; Kaltsoyannis, N. Computational Analysis of M-O Covalency in $M(OC_6H_5)_4$ (M = Ti, Zr, Hf, Ce, Th, U). *Dalton Trans.* **2019**, *48*, 2939.

For Table of Contents Use Only

Tetrahalocatecholate Rare Earth Complexes: Dinuclear Motifs with Intramolecular RE···XC(Ar) Interactions

Elodie Rousset, Robert W. Gable, Alyona Starikova, Colette Boskovic

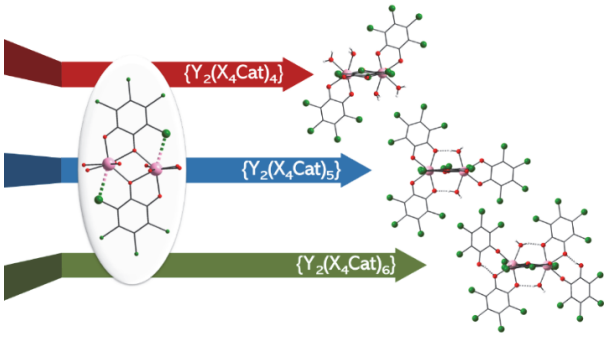

Intramolecular Y···XC(Ar) interactions play a role in generating a robust tetrahalocatecholate-bridged dinuclear yttrium core motif that is conserved across multiple complexes. Careful control of reaction and crystallization conditions allows selective isolation of the individual species. Applying these methods to redox-active cerium instead affords trinuclear mixed-valence $\{Ce^{III}Ce^{IV}_2\}$ and mononuclear cerium(IV) complexes.